ISSN 1070-3284, Russian Journal of Coordination Chemistry, 2018, Vol. 44, No. 2, pp. 117–126. © Pleiades Publishing, Ltd., 2018.
Original Russian Text © Yu.A. Bryleva, L.A. Glinskaya, K.S. Marenin, A.S. Bogomyakov, D.A. Piryazev, A.V. Tkachev, S.V. Larionov, 2018, published in Koordinatsionnaya Khimiya, 2018, Vol. 44, No. 1, pp. 28–37.

Copper(II) Complexes with Chiral Ligands Containing Fragments of Monoterpenoids and Amino Acid Esters

Yu. A. Bryleva[a, *], **L. A. Glinskaya**[a], **K. S. Marenin**[b], **A. S. Bogomyakov**[c],
D. A. Piryazev[a, d], **A. V. Tkachev**[b, d], and **S. V. Larionov**[a, d]

[a]*Nikolaev Institute of Inorganic Chemistry, Siberian Branch, Russian Academy of Sciences, pr. akademika Lavrent'eva 3, Novosibirsk, 630090 Russia*
[b]*Vorozhtsov Institute of Organic Chemistry, Siberian Branch, Russian Academy of Sciences, Novosibirsk, 630090 Russia*
[c]*International Tomography Center, Siberian Branch, Russian Academy of Sciences, Novosibirsk, 630090 Russia*
[d]*Novosibirsk National Research State University, Novosibirsk, Russia*
**e-mail: bryleva@niic.nsc.ru*

Received July 18, 2017

Abstract—Complexes $[CuL^1Cl_2]$ (**I**), $[CuL^2Cl_2] \cdot EtOH$ (**II**), and $Cu_2L^3Cl_4$ (**III**) containing esters of the N-derivatives of optically active amino acids based on (+)-3-carene (L^1, L^2) and (–)-α-pinene (L^3) are synthesized. The crystal and molecular structures of compounds **I** and **II** are determined by X-ray diffraction analyses (CIF files CCDC nos. 1560071 (**I**), 1560072 (**II**)). The crystal structure of compound **I** consists of mononuclear complex molecules. In the structure of compound **II**, the unit cell contains two crystallographically independent molecules of mononuclear complex $[CuL^2Cl_2]$ and two EtOH molecules. Ligands L^1 and L^2 perform the tridentate-chelating function by the N atoms of the NH and NOH groups and by the O atom of the C=O group. In compounds **I** and **II**, the coordination polyhedra Cl_2N_2O of the Cu atoms are trigonal bipyramid. According to the data of IR and electronic spectroscopy, binuclear complex **III** has similar coordination polyhedra. The experimental values of μ_{eff} for compounds **I**, **II**, and **III** at 300 K are 1.93, 1.88, and 2.71 μ_B. For complex **III**, the $\mu_{eff}(T)$ dependence in a range of 2–300 K indicates a weak ferromagnetic exchange interaction.

Keywords: synthesis, complex, copper(II), pinene, carene, terpene–amino acid hybrids, structure

DOI: 10.1134/S1070328418020033

INTRODUCTION

Coordination copper compounds with organic ligands belong to the well-studied classes of complex compounds. The properties of the complexes of copper in different oxidation states are diverse, and these compounds have a wide range of functional properties and areas of practical application. Copper is among the vital metals composing a series of enzymes [1–4]. The copper-containing proteins contain copper, both in the form of Cu(II) and Cu(I). A deficient or an excess of copper in the organism is related, for example, to brain diseases, oncology, and hepatitis [2, 3, 5]. Coordination metal complexes, in particular, various copper complexes with organic ligands [5–12], including chiral compounds [13], are widely used for the treatment of these diseases. The list of these copper complexes contains the compounds bearing chiral natural substances, for instance, amino acids histidine [5] and L-tyrosine [11], or amino acid fragments [7] as ligands. The synthesis of copper compounds with ligands containing moieties of other chiral biologically active natural compounds seems to be promising. In particular, the ligands bearing fragments of chiral terpenoids extracted from dendrochemical raw materials are used for the synthesis of the complexes [14–17]. For example, the cytotoxicity of the Cu(I) complexes with the camphor derivatives was studied [18].

It seems interesting to synthesize chiral metal complexes with hybrid ligands containing terpenoid fragments and amino acids. For example, the Cu(II) and Ag(I) complexes with the chiral N-derivatives of aminoacetic acid based on natural monoterpenes (+)-3-carene and (–)-α-pinene [19], as well as the Pd(II) compounds with the ligands constructed of α-pinene and β-alanine molecules [20], were obtained.

The purpose of this work is to synthesize and study the structures of the Cu(II) complexes with the earlier synthesized chiral methyl esters of (2*S*)-2-((1*S*,3*S*,6*R*,*E*)-4-hydroxyiminocaran-3-ylamino)-3-phenylpropionic (L^1) and (2*S*)-2-((1*S*,3*S*,6*R*,*E*)-4-hydroxyiminocaran-3-

ylamino)-2-phenylacetic (L^2) acids and with the new chiral ligand bis{[(1*R*,2*R*,3*E*,5*R*)-2-((1*S*)-2-phenyl-1-methoxycarbonylethylamino)pinan-3-ylidene]aminooxy}methane (L^3).

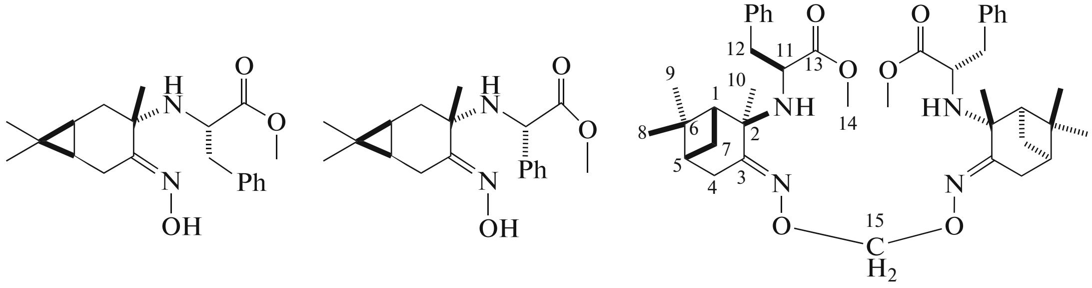

L^1 L^2 L^3

(atoms are numbered for the interpretation of NMR spectra)

Scheme 1

EXPERIMENTAL

The following reagents were used for the synthesis of compound L^3 and the complexes: $CuCl_2 \cdot 2H_2O$ (high-purity grade), EtOH (rectificate), acetone (special purity grade), CH_2Cl_2 (reagent grade), KOH (analytical grade), and $(n\text{-Bu})_4N(HSO_4)$ (high-purity grade). Compounds L^1 ($[\alpha]^{26}_{589}$ +78) and L^2 ($[\alpha]^{27}_{589}$ +165) were obtained from (+)-3-carene, and methyl (2*S*)-2-[(1*R*,2*R*,3*E*,5*R*)-3-hydroxyliminopinan-2-ylamino]-3-phenylpropionate ($[\alpha]^{26}_{589}$ –36 (*c* 0.773, EtOH)) was obtained from (–)-α-pinene using earlier described procedures [21].

Synthesis of L^3. A solution of methyl (2*S*)-2-[(1*R*,2*R*,3*E*,5*R*)-3-hydroxyliminopinan-2-ylamino]-3-phenylpropionate (10.5 mmol, 3.6 g) in CH_2Cl_2 (15 mL) was added with vigorous stirring to a boiling mixture of CH_2Cl_2 (100 mL), aqueous alkali (9 g of KOH in 10 mL of distilled water), and the phase-transfer catalyst (tetrabutylammonium hydrosulfate, 30 mg). In 5 min, heating and stirring were stopped and the organic phase was sampled for analysis by thin-layer chromatography (TLC). If the chromatogram had a spot of the starting compound, heating and stirring were resumed. After the end of the reaction (the disappearance of the spot of the starting compound according to TLC), the heating and stirring were stopped, after which distilled water (100 mL) was poured to the reaction mixture. The organic phase was separated, and the aqueous phase was singly extracted with CH_2Cl_2 (50 mL). The joined organic extract was dried over anhydrous Na_2SO_4 and evaporated in a vacuum of a water-jet pump. The crude product was dried by column chromatography. The yield was 2.56 g (70%). The white finely crystalline powder was recrystallized from MeCN, mp = 141–145°C, $[\alpha]^{29}_{589}$ –80 (*c* 0.95, $CHCl_3$).

High-resolution mass spectrum (ES, 4500 V, positive ions): found *m/z* = 701.427, for $C_{41}H_{56}N_4O_6$ calculated $[M+H]^+$ = 701.42781; found *m/z* 723.409, calculated $[M+Na]^+$ = 723.40976.

IR (ν, cm^{-1}): 3369 ν(N–H), 1725 ν(C=O), 991 ν(N–O). ^1H NMR ($CDCl_3$), δ, ppm: 7.36–7.13 (m, 5 H_{Ar}); 5.45 (s, 1 H, $C(15)H_2$); 3.76 (dd, 1 H, C(11)H, *J* = 8.3, 5.7 Hz); 3.57 (s, 3 H, $C(14)H_3$); 2.82 (dd, 1 H, $C(12)H_2$, *J* = 13.3, 5.7 Hz); 2.68 (dd, 1 H, $C(12)H_2$, *J* = 13.3, 8.4 Hz); 2.64 (ddd, 1 H, *pro-R*-C(4)H, *J* = 18.1, 2.8, 2.8 Hz); 2.33 (dd, 1 H, *pro-S*-C(4)H, *J* = 18.4, 2.5 Hz); 2.17 (dddd, 1 H, *pro-S*-C(7)H), *J* = 10.7, 6.0, 6.0, 2.8 Hz); 1.84 (s, 1 H, C(1)H); 1.83 (s, 1 H, C(5)H); 1.48 (d, 1 H, *pro-R*-C(7)H, *J* = 10.6 Hz); 1.21 (s, 3 H, $C(9)H_3$); 1.08 (s, 3 H, $C(10)H_3$); 0.71 (s, 3 H, $C(8)H_3$). ^{13}C NMR ($CDCl_3$), δ, ppm: 177.25 (C(13)); 162.70 (C(3)); 138.18, 129.37, 127.81, 126.14 (C_{Ar}); 98.02 (C(15)); 59.43 (C(2)); 56.50 (C(11)); 51.66 (C(1)); 51.44 (C(14)); 41.33 (C(12)); 39.00 (C(6)); 38.03 (C(5)); 30.73 (C(4)); 28.08 (C(7)); 27.46 (C(9)); 25.03 (C(10)); 22.52 (C(8)).

Synthesis of $[CuL^1Cl_2]$ (I). A solution of $CuCl_2 \cdot 2H_2O$ (0.051 g, 0.2 mmol) in EtOH (3 mL) was added with stirring to a solution of L^2 (0.069 g, 0.3 mmol) in EtOH (4 mL). Magnetic stirring for 1 h resulted in the formation of a blue precipitate. Then the solvent was evaporated under an air flow to 3 mL. The precipitate was filtered off, washed with cooled EtOH, and dried in a desiccator over anhydrone. The yield was 0.065 g (70%).

For $C_{20}H_{28}N_2O_3Cl_2Cu$

Anal. calcd., %	C, 50.2	H, 5.9	N, 5.8
Found, %	C, 50.0	H, 5.8	N, 5.8

IR (ν, cm^{-1}): 3188 ν(N–H), 1709 ν(C=O), 1025 ν(N–O). $[\alpha]_{589}^{31}$ +63 (*c* 0.538, CH_2Cl_2), μ_{eff} (300 K) = 1.93 μ_B, electronic reflectance spectrum of the solid sample: λ_{max} = 756 nm. Dark blue single crystals suitable for X-ray diffraction analysis were grown by the slow evaporation of a solution of complex **I** in EtOH.

Synthesis of [CuL^{2}Cl$_2$] · EtOH (II). A solution of $CuCl_2 \cdot 2H_2O$ (0.020 g, 0.12 mmol) in EtOH (3 mL) was added with stirring to a solution of L^2 (0.038 g, 0.12 mmol) in EtOH (3 mL). The obtained solution was magnetically stirred for 1 h, and then the beaker with the solution was placed in a refrigerator. In 2 days, a precipitate was formed as blue-green rectangular crystals suitable for X-ray diffraction analysis. The precipitate was filtered off, washed with cooled EtOH, and dried in a desiccator over anhydrone. The yield was 0.025 g (40%).

For $C_{21}H_{32}N_2Cl_2O_4Cu$

Anal. calcd., %	C, 49.4	H, 6.3	N, 5.5
Found, %	C, 49.4	H, 5.9	N, 5.7

IR (ν, cm^{-1}): 3195 ν(N–H), 1713 ν(C=O), 1024 ν(N–O). $[\alpha]_{589}^{30}$ +17 (*c* 0.227, EtOH), μ_{eff} (300 K) = 1.88 μ_B.

Synthesis of Cu$_2$L^{3}Cl$_4$ (III). A solution of $CuCl_2 \cdot 2H_2O$ (0.034 g, 0.2 mmol) in acetone (3 mL) was added with stirring to a solution of L^3 (0.070 g, 0.1 mmol) in acetone (5 mL). Stirring for 1 h resulted in the formation of a yellow precipitate. The precipitate was filtered off, washed with acetone, and dried in a desiccator over anhydrone. The yield was 0.048 g (50%).

For $C_{41}H_{56}N_4O_6Cl_4Cu_2$

Anal. calcd., %	C, 50.8	H, 5.8	N, 5.8
Found, %	C, 51.0	H, 5.8	N, 5.7

IR (ν, cm^{-1}): 3256 ν(N–H), 1682 ν(C=O), 1014 ν(N–O). $[\alpha]_{589}^{32}$ –164 (*c* 0.549, EtOH), μ_{eff} (300 K) = 2.71 μ_B, electronic reflectance spectrum of the solid sample: λ_{max} = 899 nm.

Microanalyses to the contents of C, H, and N were performed on a EuroEA 3000 analyzer. The Sorbfil plates (PTSKh-AF-A-UF trade mark) with the immobilized sorbent (SiO_2) layer and the UV indicator were used for TLC. The irradiation of the plates with a UV lamp and keeping in iodine vapors were used for the visualization of the components of the analyzed mixtures. Silica gel (grain size 0.050–0.160 mm, OOO Imid) were used for column chromatography. The melting point of compound L^3 was determined on a Kofler stage. Optical rotation values were measured on a PolAAr 3005 polarimeter, and the concentrations are given in g/100 mL. The mass spectrum of L^3 was detected on a Bruker micrOTOF-Q spectrometer. The IR spectrum of compound L^3 in KBr was recorded on a Bruker TENSOR 27 instrument. The IR spectra of complexes **I–III** were recorded on a VERTEX 80 spectrometer (in fluorinated oil, in a range of 4000–1500 cm^{-1}; in Nujol, at 1500–400 cm^{-1}). The NMR spectra of compound L^3 were recorded on a Bruker DRX-500 spectrometer (^{1}H, 500.13 MHz; ^{13}C, 125.77 MHz) for solutions with the concentration 5–10 mg/mL at 30°C. The signals of the solvent ($CDCl_3$) served as an internal standard: δH = 7.24 ppm, δC = 76.90 ppm.

X-ray diffraction analysis. For single crystals of compounds **I** and **II**, the unit cell parameters and reflection intensities were measured at a low temperature (150 K) on a Bruker X8 ApexCCD automated diffractometer equipped with a two-coordinate detector using a standard procedure (MoK_α radiation, λ = 0.71073 Å, graphite monochromator). The crystallographic characteristics, details of X-ray diffraction experiments, and structure refinement for compounds **I** and **II** are presented in Table 1. The structures were solved by a direct method and refined by full-matrix least squares in the anisotropic (for non-hydrogen atoms) approximation using the SHELXL-97 program package [22]. The positions of all hydrogen atoms were determined from the difference Fourier syntheses and included into the refinement in the riding model. Selected interatomic distances and bond angles are given in Table 2.

The full tables of atomic coordinates, bond lengths, and bond angles were deposited with the Cambridge Crystallographic Data Centre (CIF file CCDC nos. 1560071 (**I**), 1560072 (**II**); deposit@ccdc.cam.ac.uk or http://www.ccdc.cam.ac.uk/data_request/cif) and are available from the authors.

The X-ray phase analysis of polycrystals of complex **I** was carried out on a Shimadzu XRD-7000 diffractometer (CuK_α radiation, Ni filter, 2θ range 5°–60°, increment 0.03° 2θ, point scan 1 s). The sample for the study was prepared as follows. The polycrystals were triturated in an agate mortar in the presence of heptane, and the obtained suspension was deposited on the polished side of a standard quartz cell. After heptane drying, the sample represented a thin steady layer (thickness ~100 μm).

The magnetic susceptibility (χ) of samples of compounds **I–III** was measured on an MPM*SXL* SQUID magnetometer (Quantum Design) in a temperature range of 2–300 K at a magnetic field strength of 5 kOe. The paramagnetic components of the magnetic susceptibility were determined taking into account the diamagnetic contribution estimated from Pascal's constants. The effective magnetic moment (μ_{eff}) was calculated by the formula $\mu_{eff} = [3k\chi T/(N_A\mu_B^2)]^{1/2}$, where N_A, μ_B, and k are Avogadro's number, the Bohr magneton, and the Boltzmann constant, respectively.

Table 1. Crystallographic characteristics and the experimental and structure refinement details for compounds **I** and **II**

Parameter	Value	
	I	**II**
FW	478.88	1021.85
Crystal system	Orthorhombic	Monoclinic
Space group	$P2_12_12_1$	$P2_1$
a, Å	11.5352(4)	8.5001(3)
b, Å	11.9349(3)	14.6744(5)
c, Å	16.3601(6)	19.3018(5)
β, deg	–	100.733(1)
V, Å^3	2252.3(1)	2365.5(1)
Z; ρ_{calcd}, mg/cm^3	4; 1.412	4; 1.435
μ, mm^{-1}	1.229	1.178
Crystal sizes, mm	0.15 × 0.1 × 0.1	0.15 × 0.15 × 0.1
Scan range over θ, deg	2.11–37.95	1.75–30.50
Number of measured/independent reflections R_{int}	29907/11467 0.0735	16463/10942 0.0340
Number of reflections with $I > 2\sigma(I)$	6692	8546
Number of refined parameters	257	551
Goodness-of-fit for F^2	0.971	0.969
R_1, wR_2 ($I > 2\sigma(I)$)	0.0545, 0.0830	0.0448, 0.0770
R_1, wR_2 (for all I_{hkl})	0.1173, 0.1044	0.0654, 0.0854
Residual electron density (max/min), e/Å^3	0.56/–0.84	0.513/–0.472
Absolute structure parameter	–0.014(11)	0.004(9)

The electronic reflectance spectra of powders of pressed compounds **I** and **III** were recorded on a UV-3101PC spectrometer (Shimadzu) in a range of 240–2000 nm.

RESULTS AND DISCUSSION

Compound L^3 of the C_2 symmetry was obtained by the reaction of cross-linking of two oxime groups of bis-α-aminooximes by dichloromethane under the phase-transfer catalysis conditions described earlier [23]. The two-phase system of CH_2Cl_2 and a 40% aqueous solution of KOH with tetrabutylammonium hydrosulfate as a phase-transfer catalyst turned out to be the most efficient for the reaction to occur. The reaction was carried out with vigorous stirring at the boiling point of CH_2Cl_2 (40°C). The analysis by TLC monitoring showed that the complete conversion of the starting compound occurred in 15 min (Scheme 2).

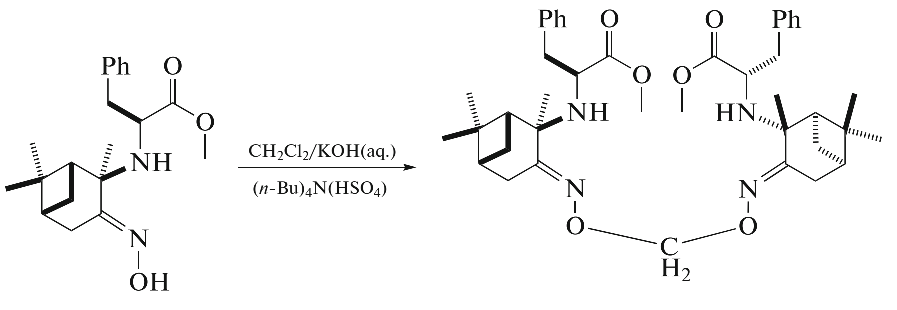

L^3

Scheme 2

The empirical formula of L^3 coincided with the expected one was established by high-resolution mass spectrometry. An analysis of the NMR spectra of the products shows the disappearance of the signals of the

Table 2. Selected interatomic distances *d* (Å) and bond angles ω (deg) in the structures of complexes **I** and **II***

I		**II**			
Bond	*d*, Å	Bond	*d*, Å	Bond	*d*, Å
Cu(1)–N(1)	1.996(2)	Cu(1)–N(1)	1.995(3)	Cu(2)–N(3)	2.024(3)
Cu(1)–N(2)	2.089(2)	Cu(1)–N(2)	2.095(3)	Cu(2)–N(4)	2.075(3)
Cu(1)–Cl(2)	2.207(1)	Cu(1)–Cl(2)	2.221(1)	Cu(2)–Cl(4)	2.231(1)
Cu(1)–Cl(1)	2.280(1)	Cu(1)–Cl(1)	2.266(1)	Cu(2)–Cl(3)	2.248(1)
Cu(1)–O(2)	2.396(2)	Cu(1)–O(12)	2.240(3)	Cu(2)–O(22)	2.220(3)
N(1)–C(4)	1.269(3)	N(1)–C(14)	1.273(4)	N(3)–C(24)	1.271(4)
N(1)–O(1)	1.393(3)	N(1)–O(11)	1.388(4)	N(3)–O(21)	1.393(4)
N(2)–C(11)	1.480(3)	N(2)–C(111)	1.487(4)	N(4)–C(211)	1.494(4)
N(2)–C(3)	1.516(3)	N(2)–C(13)	1.509(4)	N(4)–C(23)	1.505(4)
O(2)–C(13)	1.212(3)	O(12)–C(112)	1.203(4)	O(22)–C(212)	1.207(4)
O(3)–C(13)	1.319(3)	O(13)–C(112)	1.313(4)	O(23)–C(212)	1.323(4)
O(3)–C(14)	1.457(3)	O(13)–C(113)	1.450(5)	O(23)–C(213)	1.456(4)
C(3)–C(10)	1.532(4)	C(13)–C(110)	1.529(5)	C(23)–C(210)	1.545(5)
C(7)–C(8)	1.509(4)	C(17)–C(18)	1.522(6)	C(27)–C(28)	1.513(6)
C(7)–C(9)	1.512(4)	C(17)–C(19)	1.503(3)	C(27)–C(29)	1.518(5)
Angle	ω, deg	Angle	ω, deg	Angle	ω, deg
N(1)Cu(1)N(2)	78.91(8)	N(1)Cu(1)N(2)	78.1(1)	N(3)Cu(2)N(4)	77.7(1)
N(1)Cu(1)Cl(2)	161.55(7)	N(1)Cu(1)Cl(2)	156.01(9)	N(4)Cu(2)Cl(4)	168.38(9)
N(2)Cu(1)Cl(2)	95.31(6)	N(2)Cu(1)Cl(2)	92.96(8)	N(3)Cu(2)Cl(4)	91.69(9)
N(1)Cu(1)Cl(1)	89.45(6)	N(1)Cu(1)Cl(1)	90.40(9)	N(4)Cu(2)Cl(3)	90.93(9)
N(2)Cu(1)Cl(1)	167.25(6)	N(2)Cu(1)Cl(1)	168.03(9)	N(3)Cu(2)Cl(3)	153.46(9)
Cl(2)Cu(1)Cl(1)	97.35(3)	Cl(2)Cu(1)Cl(1)	98.94(4)	Cl(4)Cu(2)Cl(3)	100.69(4)
N(1)Cu(1)O(2)	83.01(9)	N(1)Cu(1)O(12)	94.9(1)	N(3)Cu(2)O(22)	96.9(1)
N(2)Cu(1)O(2)	79.29(7)	N(2)Cu(1)O(12)	79.9(1)	N(4)Cu(2)O(22)	80.2(1)
Cl(2)Cu(1)O(2)	113.38(5)	Cl(2)Cu(1)O(12)	105.45(8)	Cl(4)Cu(2)O(22)	96.61(7)
Cl(1)Cu(1)O(2)	94.25(5)	Cl(1)Cu(1)O(12)	98.05(7)	Cl(3)Cu(2)O(22)	104.75(8)

* The C–C bond lengths in the six-membered alicycles of complex **I** are 1.515(4)–1.547(3) Å, and those in the benzene ring of complex **I** are 1.380(4)–1.395(4); the C–C bond lengths in the six-membered alicycles of complex **II** are 1.517(5)–1.548(5) Å, and those in the benzene ring of complex **II** are 1.365(6)–1.397(6) Å.

oxime protons and the appearance of the signals corresponding to the acetal methylene group with the retention of all other signals of the starting substances. In the ^{1}H NMR spectrum, the relative integral intensity of signals of the protons of the methylene group is consistent with the relative integral intensities of the signals corresponding to one proton of the terpene fragment as 1 : 1. This suggests that the synthesized compound has the C_2 symmetry.

Paramagnetic chiral compounds **I**–**III** were obtained by the complex formation of $CuCl_2$ with optically active reagents L^1 and L^2 in EtOH and with L^3 in acetone. According to the elemental analysis data, the Cu to ligand ratio is 1 : 1 in the right-rotating complexes **I** and **II**, and this ratio is 2 : 1 in left-rotating complex **III**. The structure of ligand L^3 and the elemental analysis data suggest that complex **III** is binuclear.

According to the X-ray diffraction data, complex **I** is mononuclear. Its crystal structure consists of isolated acentric molecules, all atoms of which occupy the general positions (Fig. 1a). The Cu atom coordinates two N atoms, the O atom of the C=O group of tridentate-chelating ligand L^1, and two Cl atoms (coordination number 5). The coordination polyhedron Cl_2N_2O is a trigonal bipyramid with the Cl(2) and N(1) atoms in the axial vertices at distances of 2.207(2) and 1.845(2) Å, respectively, from the equatorial plane of the bipyramid. The root-mean-square deviation from the plane passed through the atoms Cu(1)N(2)O(2)Cl(1) is 0.088(1) Å. The Cu–N distances differ substantially: Cu–N of the oxime group (1.996(2) Å) is shorter than Cu–N of the imine group (2.089(2) Å). The Cu–Cl distances differ insignificantly (Table 2). The Cu–N, Cu–Cl, and Cu–O bond lengths in the complex correspond to the published data for coordination compounds of this type [24]. Two five-membered chelate cycles $CuNOC_2$ and CuN_2C_2 undergo ring closure upon the coordination of L^1 to the Cu^{2+} ion, and the dihedral angle between their planes is 86.2(1)°. Both chelate cycles have an envelope conformation: the C(3) and C(11) atoms deviate from the planes of four other atoms by 0.521(3) and –0.469(3) Å, respectively. The short intramolecular hydrogen bond O–H···Cl (O···Cl 2.970(1) Å at the sum of the van der Waals radii of Cl and O equal to 3.3 Å [25]) results in the formation of an additional five-membered H-cycle Cu(1)N(1)O(1)H(O1)Cl(1) in the envelope conformation. The Cl(1)H(O1)O(1) angle is 138°.

The six-membered carbocycle of the ligand has a distorted bath conformation, and the C(2) and C(5) atoms deviate from the plane of four atoms of the carbocycle by 0.430(4) and 0.624(4) Å. The dimethylcyclopropane fragment is adjacent to the six-membered carbocycle by the common C–C edge and forms a dihedral angle of 136.7(2)° with the plane of four C atoms. The benzene ring of the ligand is nearly planar, and the deviation from the root-mean-square plane is 0.007(2) Å.

The projection of the molecular packing of complex **I** onto the (010) plane is presented in Fig. 1b. The intermolecular distances range within the van der Waals interactions and weak hydrogen bonds (Cl(2)···C(14) 3.466(2) Å) [25].

The theoretical diffraction pattern calculated from the X-ray diffraction data of a single crystal of compound **I** coincided with the experimental diffraction pattern of this complex obtained from the polycrystalline phase (Fig. 2). This indicates that the synthesis product and single crystal have the same structures.

The unit cell of the crystal structure of compound **II** contains two crystallographically independent molecules 1 and 2 of the mononuclear complex and two solvate molecules of EtOH. The structure of one of two independent but similar molecules of the complex is shown in Fig. 3a.

The complex in compound **II** has the molecular structure similar to that of compound **I**. The Cu–N, Cu–Cl, and Cu–O interatomic distances in complexes **I** and **II** differ insignificantly (Table 2). The coordination polyhedra of the Cu atoms in complexes **I** and **II** are the same. As in complex **I**, two five-membered chelate cycles undergo ring closure upon the coordination of L^2 to the Cu^{2+} ion in complex **II**. The dihedral angles between the planes of the cycles are 78.7(1)° in molecule 1 and 77.4(1)° in molecule 2. The CuN_2C_2 chelate cycles have the envelope conformation: the C(13) and C(23) atoms deviate from the planes of four other atoms by –0.593(5) and 0.615(5) Å, respectively. The $CuNOC_2$ cycles are almost planar, and the deviations from the root-mean-square planes are 0.008(2) (molecule 1) and 0.039(2) Å (molecule 2). In complex **I**, unlike complex **II**, the $CuNOC_2$ cycle has the envelope conformation. The five-membered H-cycle Cu(1)N(1)O(11)-H(O11)Cl(1) in the envelope conformation is formed in the structure of each molecule of complex **II**, as in complex **I**, due to the short intramolecular hydrogen bond O–H···Cl (O···Cl 3.018(1) Å in molecule 1 and 3.097(1) Å in molecule 2).

The six-membered carbocycle has the conformation of a distorted bath, and the C(12), C(15), C(22), and C(25) atoms deviate from the plane of four atoms of the carbocycle by –0.410(5), –0.612(5), 0.384(6), and 0.604(6) Å, respectively. The dimethylcyclopropane fragment is adjacent to the six-membered carbocycle by the common edge C–C and forms dihedral angles of 135.5(3)° (molecule 1) and 135.1(3)° (mole-

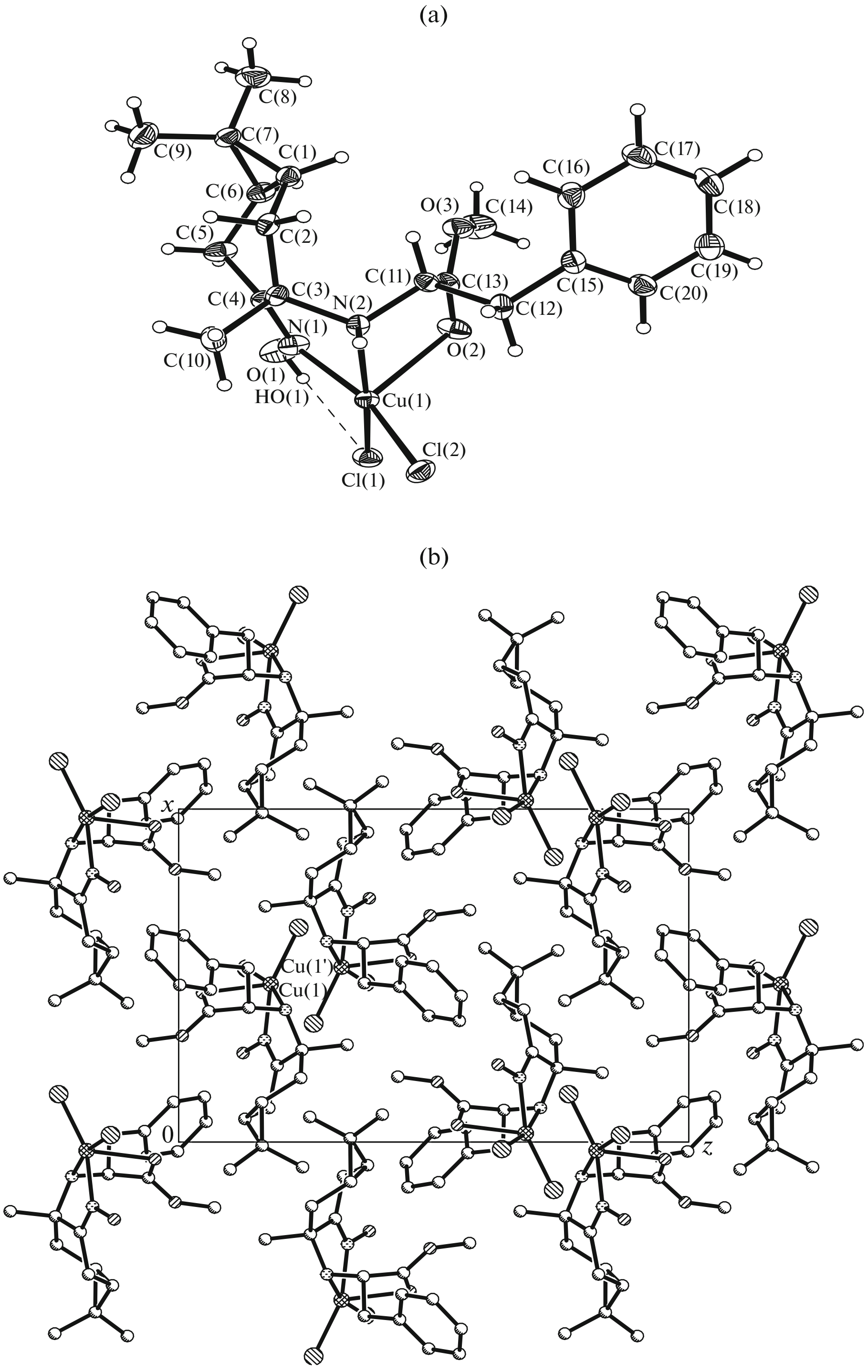

Fig. 1. (a) Molecular structure of complex **I** and (b) the projection of the molecular packing of complex **I** onto the (010) plane. Hydrogen atoms are omitted.

cule 2) with the plane of four C atoms. The benzene rings are also nearly planar, and the deviation from the root-mean-square planes are 0.006(3) and 0.008(3) Å in molecules 1 and 2, respectively.

The packing of molecules of the complex and EtOH molecules in the crystal structure of compound **II** is presented in the projection onto the (010) plane (Fig. 3b). The shortest distances between the Cl atoms of the complex and adjacent EtOH molecules (Cl(3)···O(2C) 3.230(3) Å) are at the level of van der Waals interactions and weak hydrogen bonds Cl···H–C [25]. Therefore, intermolecular interactions are fairly weak.

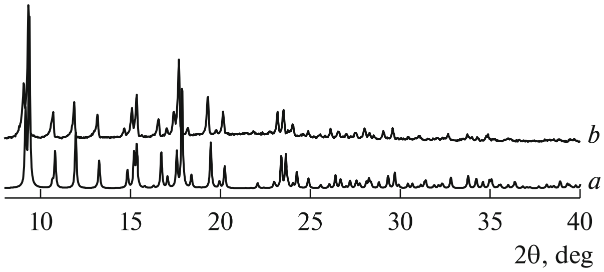

Fig. 2. (*a*) Theoretical and (*b*) experimental diffraction patterns of complex **I**.

A comparison of the crystal structures of compounds **I** and **II** showed that the difference in the structures of L^1 and L^2 substantially changed the packing in the structure of compound **II**. The unit cell parameters change, and the space group decreases. As a consequence, the minimum Cu···Cu distance increases significantly. This distance in the structure of compound **I** is equal to 6.414(1) Å, whereas in compound **II** the Cu···Cu distances are 7.565(2) Å for Cu(1)···Cu(2), 8.218(1) Å for Cu(2)···Cu(2), and 8.349(2) Å for Cu(1)···Cu(1). It is most likely that the significant distance between the molecules of the complex in the structure of compound **II** favored the formation of a solvate.

In the IR spectra of compounds **I** and **II**, the ν(N–H) (~3188), ν(C=O) (~1711), and ν(N–O) (~1025 cm^{-1}) bands are shifted compared to the position of these bands in the spectra of free ligands L^1 and L^2: ν(N–H) (3296 and 3313), ν(C=O) (1734 and 1722), and ν(N–O) (949 and 932 см^{-1}) for L^1 and L^2, respectively, presented in [21]. The shift of these bands agrees with the character of coordination of L^1 and L^2 according to the X-ray diffraction data for compounds **I** and **II**.

The ν(N–H), ν(C=O), and ν(N–O) bands in the IR spectrum of binuclear complex **III** are also shifted relative to the positions of the bands in the spectrum of free ligand L^3. They are rather close to the found values of frequencies in the spectra of mononuclear complexes **I** and **II**, whose structures were determined by X-ray diffraction analysis. It is most likely that in complex **III** the Cu atoms have the same coordination environment Cl_2N_2O as in compounds **I** and **II** (the coordination number of Cu is 5).

The colors of the solid phases of complexes **I** and **II**, which contain the trigonal bipyramidal unit-chromophores $CuCl_2N_2O$, differ slightly. The band maximum of the *d*–*d* transition at 756 nm (13200 cm^{-1}) in the electronic reflectance spectrum of compound **I** lies in the energy range characteristic of the complexes of Cu^{2+} ions having the trigonal bipyramidal structure of the chromophore [26]. The experimental values of μ_{eff} at 300 K for mononuclear complexes **I** and **II** equal to 1.93 and 1.88 μ_B, respectively, are slightly higher than the single spin value of μ_{eff} (1.73 μ_B) for the Cu^{2+} ion. This indicates the contribution of the orbital moment.

The color of complex **III** (yellow) differs strongly from the color of complexes **I** and **II**. The band in the electronic reflectance spectrum ($\lambda_{\text{max}} = 899$ nm, $\nu = 11100\ \text{cm}^{-1}$) is shifted to lower energies compared to the position of the band in the electronic reflectance spectrum of complex **I**. At the same time, this band lies in the energy range characteristic of the trigonal bipyramidal complexes of Cu^{2+} ions. It is most likely that complex **III** also has the trigonal bipyramidal units $CuCl_2N_2O$, which are possibly somewhat distorted as compared to the units of complexes **I** and **II**. The experimental value of μ_{eff} for complex **III** is 2.67 μ_B at 300 K and remains almost unchanged with a decrease in the temperature to 20 K, after which increases slightly (to 2.72 μ_B) at 5 K (Fig. 4). The $1/\chi(T)$ dependence is linear and obeys the Curie–Weiss law with the optimum values of parameters *C* and θ equal to 0.892 K cm^3/mol and –0.09 K, respectively. The value of Curie constant *C* is consistent with the theoretical value equal to 0.867 K cm^3/mol for the complex containing two Cu^{2+} ions with a *g*-factor of 2.15. An increase in μ_{eff} at low temperatures indicates weak ferromagnetic exchange interactions. The $\mu_{\text{eff}}(T)$ dependence was examined using the model of exchange-coupled dimer. The optimum values of the *g*-factor and exchange interaction parameter *J* are 2.175 and 0.29 cm^{-1}, respectively.

Thus, the obtained results showed the possibility of synthesizing the chiral Cu(II) complexes with esters of the N-derivatives of optically active amino acids based on (+)-3-carene and (–)-α-pinene. These compounds are interesting for the further study of their biological activity.

ACKNOWLEDGMENTS

The authors are grateful to N.I. Alferova for IR spectra recording, N.P. Korotkevich for X-ray phase data, A.P. Zubareva and O.S. Koshcheeva for elemen-

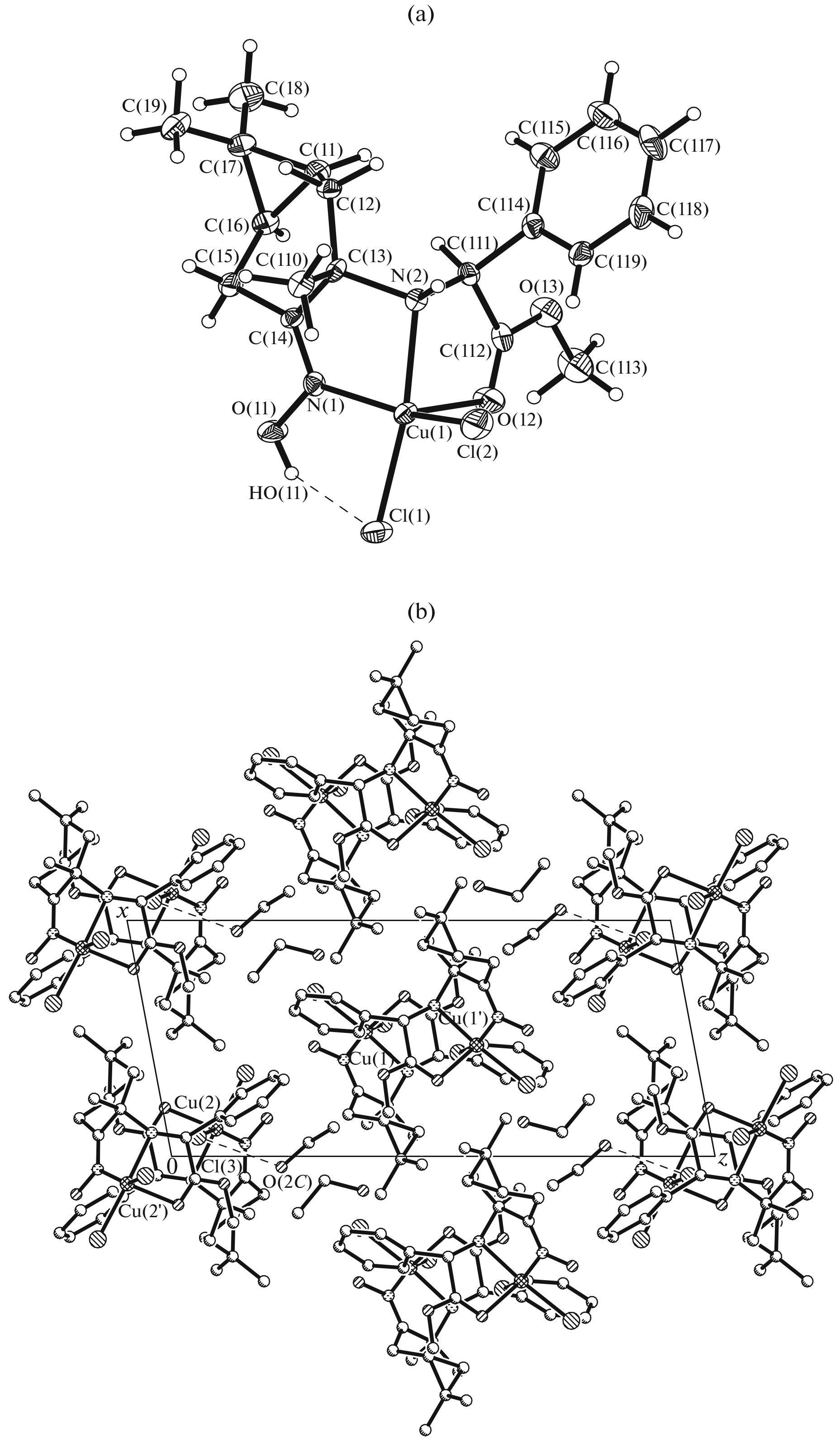

Fig. 3. (a) Molecular structure of complex **II** and (b) the projection of the molecular packing of complex **II** onto the (010) plane. Hydrogen atoms are omitted.

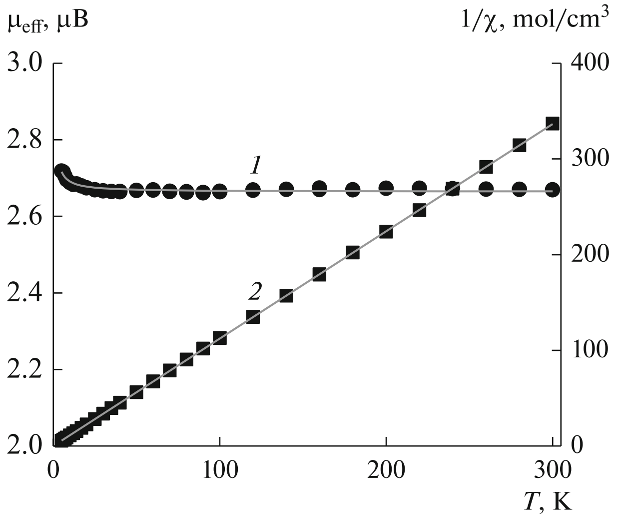

Fig. 4. Temperature dependences of (*1*) μ_{eff} and (*2*) 1/χ for complex **III**. Theoretical curves are shown by solid lines.

tal analysis data, and I.V. Yushina for electronic reflectance spectra recording.

This work was supported by the Russian Foundation for Basic Research (project no. 16-33-00696) and the President of the Russian Federation (grant for leading scientific schools no. NSh-7178.2016.3).

REFERENCES

1. Williams D.R., *The Metals of Life: The Solution Chemistry of Metal Ions in Biological Systems*, London: Van Nostrand-Reinhold, 1971.
2. Nozdryukhina, L.R. *Biologicheskaya rol' mikroelementov v organizme zhivotnykh i cheloveka* (Biological Role of Trace Minerals in the Animal and Human Body), Moscow: Nauka, 1977.
3. Hughes, M.N., *Inorganic Chemistry of Biological Processes*, Chichester: Wiley, 1981.
4. Armaroli, N., Accorsi, G., Cardinali, F., and Listorty, A., *Top. Curr. Chem.*, 2007, vol. 280, p. 69.
5. Dabrowiak, C.D., *Metals in Medicine*, New York: Wiley, 2009.
6. Marzano, C., Pellei, M., Tisato, F., and Santini, C., *Anti-Cancer Agents Med. Chem.*, 2009, vol. 9, no. 2, p. 185.
7. Santini, C., Pellei, M., Gandin, V., et al., *Chem. Rev.*, 2014, vol. 114, p. 815.
8. Blower, P.J., *Annu. Rep. Progr. Chem. A*, 2003, vol. 99, p. 589.
9. Krajc̆ova, D., Melnik, M., Havránec, E., et al., *J. Coord. Chem.*, 2014, vol. 67, no. 9, p. 1493.
10. Donnelly, P.S., *Dalton Trans.*, 2011, vol. 40, no. 5, p. 999.
11. Garbutcheon-Singh, K.B., Grant, M.P., Harper, B.W., et al., *Curr. Top. Med. Chem.*, 2011, vol. 11, p. 521.
12. Allardyce, C.S. and Dyson, P.J., *Dalton Trans.*, 2016, vol. 45, no. 8, p. 3201.
13. Sharma, S., Chauhan, M., Jamsheera, A., et al., *Inorg. Chim. Acta*, 2017, vol. 458, p. 8.
14. Zelewsky, A. and Mamula, O., *Dalton Trans.*, 2000, no. 8, p. 219.
15. Mamula, O. and von Zelewsky, A., *Coord. Chem. Rev.*, 2003, vol. 242, p. 87.
16. Larionov S.V. and Tkachev A.V., *Ros. Khim. Zh.,* 2004, vol. 48, no. 4, p. 154.
17. Larionov S.V., *Russ. J. Coord. Chem.*, 2012, vol. 38, no. 1, p. 1.
18. Fernandes, T.A., Mendes, F., Roseiro, A.P.S., et al., *Polyhedron*, 2015, vol. 87, p. 215.
19. Kokina, T.E., Agafontsev, A.M., Marenin, K.S., et al., *Koord. Khim.*, 2015, vol. 41, no. 10, p. 604.
20. Kokina, T.E., Glinskaya, L.A., Marenin, K.S., et al., *Koord. Khim.*, 2017, vol. 43, no. 4, p. 212.
21. Marenin, K.S., Gatilov, Yu.V., Agafontsev, A.M., Tkachev, A.V., *Steroids*, 2017, vol. 117, p. 112.
22. Sheldrick, G.M., *SHELX-97 Programs for Crystal Structure Analysis (Release 97–2)*, Göttingen: Univ. of Göttingen, 1997.
23. Petukhov, P.A., Bagryanskaya, I.Yu., Gatilov, Yu.V., and Tkachev, A.V., *Mend. Commun.*, 2000, vol. 10, no. 6, p. 209.
24. Kokina, T.E., Klevtsova, R.F., Glinskaya L.A., et al., *Izv. Akad. Nauk, Ser. Khim.*, 2010, no. 4, p. 698.
25. Batsanov, S.S., *Zh. Neorg. Khim.*, 1991, vol. 36, no. 12, p. 3015.
26. Lever, A.B.P., *Inorganic Electronic Spectroscopy*, Amsterdam: Elsevier, 1984.

Translated by E. Yablonskaya